HHS Public Access

Author manuscript

Mol Reprod Dev. Author manuscript; available in PMC 2016 June 11.

Published in final edited form as:

Mol Reprod Dev. 2016 February ; 83(2): 124–131. doi:10.1002/mrd.22600.

Nop2 Is Required for Mammalian Preimplantation Development

Wei Cui[1], **Jason Pizzollo**[1], **Zhengbin Han**[1,2], **Chelsea Marcho**[1], **Kun Zhang**[3], and **Jesse Mager**[1,*]

[1]Department of Veterinary and Animal Sciences, University of Massachusetts, Amherst, Massachusetts

[2]Harbin Institute of Technology, School of Life Science and Technology, Harbin, China

[3]Laboratory of Mammalian Molecular Embryology, Institute of Animal Genetics, Breeding and Reproduction, College of Animal Sciences, Zhejiang University, Hangzhou, China

SUMMARY

Nucleolar protein 2 (NOP2) is evolutionarily conserved from yeast to human, and has been found to play an important role in accelerating cell proliferation, cell-cycle progression, and tumor aggressiveness. The expression pattern and function of *Nop2* during early mammalian embryo development, however, has not been investigated. We identified *Nop2* as an essential gene for development to the blastocyst stage while performing an RNA interference (RNAi)-based screen in mouse preimplantation embryos. *Nop2* is expressed throughout preimplantation development, with highest mRNA and protein accumulation at the 8-cell and morula stages, respectively. RNAi-mediated knockdown of *Nop2* results in embryos that arrest as morula. NOP2-deficient embryos exhibit reduced blastomere numbers, greatly increased apoptosis, and impaired cell-lineage specification. Furthermore, knockdown of *Nop2* results in global reduction of all RNA species, including rRNA, small nuclear RNA, small nucleolar RNA, and mRNA. Taken together, our results demonstrate that *Nop2* is an essential gene for blastocyst formation, and is required for RNA processing and/or stability in vivo during preimplantation embryo development in the mouse.

INTRODUCTION

The fertilized egg progresses through three major transcriptional and morphogenetic events during preimplantation embryo development, resulting in the first cell-lineage decision and formation of a blastocyst-stage embryo capable of implantation. The first event is the maternal-to-zygotic transition, which includes the degradation of maternal transcripts in favor of zygotic transcripts; this process initiates the dramatic reprogramming required for successful embryo development (Latham et al., 1991). In mice, zygotic genome activation begins in 1-cell stage embryos, but becomes obvious at the 2-cell stage (Schultz, 2002). The second major event is embryo compaction, which involves the flattening of blastomeres against each other starting at the 8-cell stage in the mouse. Compaction is accompanied by

*Corresponding author: University of Massachusetts, Amherst, 661 North Pleasant Street, Amherst, MA 01003. jmager@vasci.umass.edu.

biochemical changes involving cellular metabolism and ion transport, and results in early embryonic cells first resembling somatic cells (Fleming et al., 2001; Zeng et al., 2004). The third major event is blastomere allocation and the first cell-fate determination, where blastomeres of the morula give rise to the inner cell mass, from which the embryo proper is derived, versus the trophectoderm, from which extra-embryonic tissues are derived (Yamanaka et al., 2006). Overt, detectable gene expression patterns occur within these two distinct lineages in the compacted morula. For example, the transcription factor POU5F1 (OCT4) is enriched in the inner cell mass, where it promotes pluripotency and inhibits differentiation, although the transcription factor CDX2 becomes highly upregulated in the trophectoderm, where it influences epithelial differentiation. Appropriate regulation of POU5F1 and CDX2 are necessary for successful blastocyst formation (Cockburn and Rossant, 2010; Marcho et al., 2015).

We are currently performing an RNA interference (RNAi)-based screen, using the mouse preimplantation embryo, to understand which genes are functionally required for early embryo development (Maserati et al., 2011; Zhang et al., 2013a,b). Microinjection of long, double-stranded RNA (dsRNA) against specific transcripts into fertilized 1-cell zygotes is a robust approach to achieve gene-specific silencing (Svoboda et al., 2000; Wianny and Zernicka-Goetz, 2000) without an interferon response or significant off-target effects (Stein et al., 2005). One goal of our screen was to identify genes with previously unknown functions during preimplantation development. One of these genes encodes nucleolar protein 2 (NOP2).

Murine NOP2 is homologous to yeast protein NOP2p and human NOP2 (also named NSUN1 or P120) (de Beus et al., 1994; Mitrecic et al., 2008). NOP2 belongs to the NOP2/SUN (NSUN) RNA-methyltransferase family, which includes six other members: NSUN2 through NSUN7 (Blanco and Frye, 2014). NOP2 promotes mouse fibroblast growth and tumor formation (Perlaky et al., 1992), and is highly expressed in diverse tumor types but not in normal cells. Therefore, NOP2 is being pursued as a prognostic marker for cancer aggressiveness (Saijo et al., 2001; Bantis et al., 2004). Limited studies in mammals have demonstrated expression of *Nop2* in brain tissue and fetal liver (Wang et al., 2014; Kosi et al., 2015), but the expression pattern and function of *Nop2* during preimplantation development have not yet been investigated.

Here we show that *Nop2* is expressed throughout preimplantation development, with highest transcription and protein accumulation at the 8-cell and morula stages, respectively. We further demonstrate that NOP2 is necessary for successful preimplantation embryo development, as NOP2-deficient embryos cannot form blastocysts, arresting at the morula stage with severe cell death, impaired lineage specification, and a global reduction in RNA.

RESULTS

Expression of *Nop2* During Preimplantation

Immunofluorescence analysis during all stages of preimplantation development revealed that NOP2 protein abundance was low during the oocyte-to-2-cell embryo development period, with no obvious difference between the cytoplasm and nucleus (Fig. 1A). NOP2 abundance

increased significantly from the 4-to 8-cell stage, mostly concentrated in the nucleus, specifically around the nucleolus. NOP2 protein accumulation peaked at the morula stage, with a slight qualitative decrease in nuclear intensity in blastocyst embryos.

Quantitative and reverse-transcription PCR revealed that *Nop2* mRNA is expressed at relatively low levels in oocytes and zygotes, increased through subsequent cleavage stage divisions, peaked at the 8-cell stage, and dramatically declined in morula and blastocysts (Fig. 1B and C). This mRNA expression profile is consistent with the dynamic protein levels that we detected, although there was a slight delay between peak mRNA and protein levels, which may reflect timing of translation within each cell.

Efficient Knockdown of NOP2 by dsNop2 RNA Microinjection

dsNop2 RNA was injected into the cytoplasm of zygotes to deplete NOP2 activity. In all experiments presented, control embryos were injected with dsGFP to stimulate the RNAi machinery. Injection of specific dsNop2 RNA resulted in a drastic degradation of *Nop2* mRNA in all stages examined (Fig. 1D). Similarly, immunofluorescence analysis revealed obvious protein reduction in NOP2-knockdown embryos (hereafter referred to as dsNop2 embryos) at the morula stage (Fig. 1E), indicating successful functional loss of NOP2.

NOP2 is Required for Blastocyst Formation

We next evaluated the impact of dsNop2 microinjection on developmental progression at 24 hr (2-cell stage), 48 hr (4/8-cell stage), 72 hr (morula stage), and 96 hr (blastocyst stage) post-fertilization. In these time-course experiments, dsNop2 embryos develop to the morula stage and compact without obvious differences in morphology or rate of development compared to control dsGFP embryos (Fig. 2A). At 96 hr, 95% (103/108) of control embryos reach the blastocyst stage whereas nearly all dsNOP2 embryos—1.5% (2/105)—failed to reach the blastocyst stage (Fig. 2A and B). Some dsNop2 embryos also exhibited visible signs of degeneration at 96 hr, specifically displaying morphological irregularities (Fig. 2A, arrows).

As dsNop2 embryos cannot develop into blastocysts, we performed more-detailed analyses at the morula stage, when they still appear morphologically normal. dsNop2 embryo blastomeres appeared to compact, although we observed a reduction in the blastomere number per embryo compared to that of control embryos at 72 hr (28.2 ± 0.7 cells per dsGFP embryo; 14.9 ± 0.2 cells per dsNop2 embryo) (Fig. 2C).

We also injected a control and six distinct commercial siRNAs designed against NOP2 (Fig. 2G) in order to confirm that the observed phenotype is specifically due to the loss of NOP2 function. siRNA controls elicited no phenotype—92% (11/12) of injected zygotes form blastocysts (left most image) (Fig. 2H)—whereas none (0/69) of the Nop2 siRNA-injected embryos formed blastocysts, regardless of which siRNA was used. Thus, the arrested-development phenotype can be attributed specifically to the loss of NOP2 function.

NOP2 Deficiency Results in Apoptosis and Impaired Lineage Specification

Markers of apoptosis (active tumor protein p53 (TP53)) and lineage specification (POU5F1, for the inner cell mass, and CDX2, for the trophectoderm) were examined by immunofluorescence to understand howNOP2knockdown related to blastocyst failure. Compared with dsGFP morula at 72 hr, POU5F1 and CDX2 were greatly decreased whereas active TP53 was present in many blastomeres of dsNop2 morula (Fig. 2D). dsGFP embryos formed blastocysts with clear lineage-specific POU5F1/CDX2 localization and no detectable active TP53 after 96 hr in culture (Fig. 2E). dsNop2 embryos, on the other hand, remained arrested at the morula stage, with no lineage-specific segregation of POU5F1 or CDX2: POU5F1 was present at low levels in most blastomeres, and few blastomeres had detectable CDX2. Apoptotic cells were also more abundant and many more cells contained apoptotic bodies (Fig. 2E, arrow). An extra 12 hr of culture (108 hr total) resulted in even lower POU5F1 and CDX2 protein as well as severe aggregation of apoptotic bodies in dsNop2 embryos (Fig. 2F, arrows), indicating the death of blastomere.

NOP2 Deficiency Results in Global Reduction of RNA

NOP2 plays a role in RNA stability (Hong et al., 1997; Gustafson et al., 1998; Castello et al., 2012; Blanco and Frye, 2014), so we assessed global levels of different types of RNA in control and dsNOP2 embryos. Total RNA was isolated from identical numbers of dsGFP and dsNop2 morulae (10 each), and then assessed by bioanalyzer. Electropherograms showed that normal representative peaks of tRNA/5S/5.8S, 18S, and 28S are clearly visible in dsGFP control embryos, but were drastically decreased or entirely absent in dsNop2 embryos (Fig. 3A), suggesting a global RNA reduction following NOP2 knockdown. Pyronin Y, a fluorescent RNA dye that binds to both RNA and DNA, was also used to evaluate global RNA levels in morula. Consistent with the bioanlyzer data, an obvious decrease in Pyronin Y signal was observed in dsNop2 embryos compared with dsGFP controls (Fig. 3B).

We also performed quantitative PCR to assess the changes to several different classes of RNAs, and confirmed that rRNA (*18S*), small nuclear RNA (*Rnu6*), small nucleolar RNA (*Snord65*), and mRNAs (*Actb, Gapdh, Pou5f1, Cdx2*, and *Bax*) were all significantly reduced after NOP2 knockdown. Conversely, *Tp53* abundance was much higher, which is consistent with the active apoptosis resulting from the depletion of NOP2.

DISCUSSION

In the present study, we tracked the expression of the mammalian *Nop2* gene during preimplantation development, and demonstrated its indispensible role in early embryos. *Nop2* mRNA abundance increases at the 2-cell stage and peaks at the 8-cell stage (Fig. 1B and C), indicating that the embryonic source is the zygotic genome rather than maternal stores from the oocyte. The dynamic decline of *Nop2* mRNA after the 8-cell stage (Fig. 1B and C) suggests there is a tightly regulated mechanism that restricts its accumulation at later stages.

NOP2 promotes cell proliferation and ribosome assembly, and high NOP2 expression leads to tumor aggressiveness (Perlaky et al., 1992; Saijo et al., 2001; Bantis et al., 2004). We therefore speculate that the preimplantation expression pattern of *Nop2* is orchestrated with the dynamics of preimplantation development: For example, its levels are highest when cleavage is required, but the gene is silenced when lineage differentiation occurs. Although, we detected the majority of NOP2 protein around the nucleolus, a cytoplasmic form was also detectable. Careful observation of dsNop2 embryos (Fig. 1E) indicates that this cytoplasmic signal is not due to non-specific background; indeed, similar cytoplasmic localization has been reported in yeast (de Beus et al., 1994), suggesting that NOP2 participates in cytoplasmic events in addition to its reported role in rRNA synthesis and methylation.

dsRNA-mediated knockdown of NOP2 was used to define its function during early embryo development (Fig. 1D and E). dsNop2 embryos do not develop past the morula stage (Fig. 2A and B), indicating an indispensable role for NOP2 during blastocyst development. Blastomere number was significantly reduced in dsNop2 embryos that reach the morula stage, extending the role for NOP2 in cell proliferation and cell-cycle progression that has been reported in yeast (Hong et al., 1997) and human cancer cells (Saijo et al., 2001; Bantis et al., 2004; Wang et al., 2014) to mammalian preimplantation embryos. Blastomere number can limit blastocyst formation (Yamanaka et al., 2006; Marikawa and Alarcon, 2009), so the fewer blastomeres surviving in morulae may be one source of the lower blastocyst rates. But dsNOP2 embryos also fail to activate and properly partition the transcription factors required for inner cell mass (POU5F1) and trophectoderm (CDX2) differentiation (Figs. 2 and 3). Since *Cdx2* is essential for trophectoderm formation (Biggers et al., 1988; Watson et al., 1990), we speculate that failure to specify this lineage is another major contributor to the dsNop2 failed-blastocyst phenotype.

NOP2 in HeLa cells has also been identified as a RNA-binding protein that regulates both rRNA (Gustafson et al., 1998) and mRNA (Castello et al., 2012). We therefore analyzed global RNA levels, and found a significant reduction in all RNA types in embryos lacking NOP2 using global and gene-specific assessments (Fig. 3). The direct consequences of NOP2 loss on global levels of cellular RNAs are difficult to identify since dsNOP2 embryos are stalled or dying. Even though dsNOP2 morula appear morphologically normal, it is possible that its blastomeres are already severely compromised and thus the global RNA reduction is not specific to the loss of NOP2. On the other hand, our results are consistent with a recent study demonstrating that NOP2 interacts with and stabilizes *lncRNA-hPVT1* in human liver cancers (Wang et al., 2014).

In sum, *Nop2* is expressed during mouse preimplantation, with highest mRNA and protein accumulation at 8-cell and morula stages, respectively; is essential for blastocyst formation, as NOP2-deficient embryos arrest at the morula stage with severe apoptosis and impaired cell-lineage specification; and plays an important role in RNA processing and/or stability during early embryogenesis, as *Nop2* knockdown leads to a global reduction of diverse RNA species. Thus, NOP2 production in early cleavage stages is required for blastocyst formation.

MATERIALS AND METHODS

Embryo Recovery and Culture

Use of vertebrate animals for embryo production was approved by the Institutional Animal Care and Use Committee of the University of Massachusetts, Amherst.

B6D2F1 female mice 8–10 weeks old were induced to superovulate with 5 IU pregnant mare serum gonadotropin (Sigma-Aldrich, St. Louis, MO), followed 48 hr later by 5 IU human chorionic gonadotropin (hCG) (Sigma-Aldrich, St. Louis, MO). Superovulated females were mated with B6D2F1 males, and euthanized at 20 hr post-hCG injection for zygote collection from the oviducts. Oviductal ampullae were dissected to release zygotes, and cumulus cells were removed by pipetting in M2 medium containing hyaluronidase (EMD Millipore, Billerica, MA). Zygotes were then washed in M2 medium (EMD Millipore, Billerica, MA) and cultured in KSOM medium (EMD Millipore, Billerica, MA) at 37°C in a humidified atmosphere of 5% CO_2/5% O_2 balanced with N_2.

Preparation of dsRNA

DNA templates for T7 RNA polymerase-mediated dsRNA production were amplified from genomic DNA or preimplantation embryo cDNA using primers containing T7 binding sequences followed by gene-specific sequences for dsGFP (5′-TAATACGACTCACTATAGGGCACATGAAGCAGCACGACTT and 5′-TAATACGACTCACTATAGGGTGCTCAGGTAGTGGTTGTCG) or dsNop2 (5′-TAATACGACTCACTATAGGGGGAGCATGAGCGGATCTTAG and 5′-TAATACGACTCACTATAGGGTCCACCGTAATGGAACAGGT).

PCR products were purified using a QIAquick PCR Purification Kit (Qiagen, Hilden, Germany). In vitro transcription was performed using a MEGAscript T7 Kit (Ambion, Waltham, MA), followed by the addition of TURBO RNase-free DNase to degrade the DNA template. dsRNA was then passed through NucAway Spin Columns (Ambion, Waltham, MA) to remove salt and unincorporated nucleotides. dsRNA was extracted with phenol/chloroform (Sigma-Aldrich, St. Louis, MO), precipitated with 70% ethanol, and resuspended in RNase-free water (Integrated DNA Technologies, Coralville, IA). The quality of dsRNA was confirmed by electrophoresis both after in vitro transcription and after final precipitation. The dsRNA concentration was measured using a NanoDrop (Thermo Scientific, Waltham, MA). Each dsRNA was diluted to 2 μg/μl, and stored at −80°C until use.

siRNA Production and Sequences

The sources and sequences of all siRNAs are listed in Table 1. Five to ten picoliters of 100 μM control or Nop2 siRNA were microinjected into the cytoplasm of zygotes.

Microinjection

Microinjection was performed in M2 medium using a Nikon inverted microscope equipped with a piezo-driven (Sutter Instrument, Novato, CA) micromanipulator (TransferMan NK2, Eppendorf, Hamburg, Germany). A volume of 5–10 pl of dsNop2 (2 μg/μl) or *Nop2* siRNA

(100 μM) was microinjected into the cytoplasm of zygotes using a blunt-ended pipette of 6–7 μm in diameter. The same concentration and volume of dsGFP or scrambled siRNA was injected as a control in all experiments. After microinjection, zygotes were washed with M2 and cultured in KSOM medium at 37°C in a humidified atmosphere of 5% CO_2/5% O_2 balanced with N_2.

RNA Extraction, Reverse Transcription PCR, and Quantitative PCR

Total RNA extraction was performed with a High Pure RNA Isolation Kit (# 11828665001, Roche, Basel, Switzerland). cDNA was synthesized using an iScript cDNA synthesis kit (Bio-Rad Laboratories, Hercules, CA, 170-8891). Specific reverse-transcription primers for *Rnu6* and *Snord65*, accompanied with TaqMan probes (Life Technologies, Carlsbad, CA), were used during cDNA synthesis.

Intron-spanning primers were used for standard reverse-transcription PCR (*Actb*: 5′-GGCCCAGAGCAAGAGAGGTATCC and 5′-ACGCACGATTTCCCTCTCAGC; *Nop2*: same as for the preparation of dsNop2 T7 template, listed above). Quantitative PCR was performed on a Stratagene MX3005p using TaqMan Gene Expression Assays (Life Technologies, Carlsbad, CA) and PerfeCTa qPCR Mix with low ROX (Quanta Biosciences, Gaithersburg, MD)-based reactions. *Nop2* expression in different embryo stages was normalized to *Gapdh*. Quantification of gene expression differences between control and NOP2-knockdown groups was achieve using one-embryo-equivalent of cDNA per reaction since the knockdown of NOP2 can induce global RNA, including those encoding housekeeping genes.

All PCR reactions were run with a minimum of three replicates under the following conditions: 1 cycle of 50°C for 30 sec; 1 cycle of 95°C for 2min; then 40 cycles of 15 sec at 95°C and 30 sec at 60°C. The TaqMan probes used included: *Nop2*, Mm00663137_g1; *Gapdh*, 4352339E; *Actb*, 4352341E; *Pou5f1*, Mm00658129_gH; *Cdx2*, Mm01212280_m1; *18S*, Hs99999901_s1; *Rnu6* (U6 small nuclear RNA, also named U6 snRNA), TM1973; *Snord65* (small nucleolar RNA 65, also named snoRNA 135), TM1230, *Trp53* Mm01731287_m1; and *Bax*, Mm00432050_m1.

Pyronin Y RNA Staining

Embryos were fixed in 4% paraformaldehyde in phosphate-buffered saline (PBS) for 20 min at 25°C, washed three times in PBS containing 0.3% polyvinylpyrrolidone (PBS/PVP), and stained with 4′,6-diamidino-2-phenylindole (DAPI). Embryos were then transferred to PBS/PVP containing 5 μM Pyronin Y (Thermo Scientific, Waltham, MA) for 10 min. Stained embryos were washed three times in PBS/PVP before mounting and observation by epifluorescence illumination on an Eclipse-Ti microscope (Nikon, Tokyo, Japan).

Immunofluorescence

Embryos were fixed in 4% paraformaldehyde in PBS for 30 min, washed three times in wash buffer (PBS containing 0.1%Triton X-100), and permeabilized with PBS containing 0.5% TritonX-100 for 15 min. Embryos were then blocked for 1 hr in blocking buffer (PBS containing 10% fetal calf serum and 0.1%Triton X-100), and then incubated overnight at

4°C with primary antibodies diluted in blocking buffer. After three rinses with wash buffer, embryos were incubated for 1 hr with secondary antibodies (Alexa Fluor, Life Technologies, Carlsbad, CA) diluted 1:600 in blocking buffer. DAPI was used to stain nuclear DNA for blastomere counting. Embryos were washed three times with wash buffer, and then mounted and observed with the Eclipse-Ti microscope (Nikon, Tokyo, Japan). Identical image-capture settings were maintained for imaging all embryos. Negative-control embryos were processed without primary antibodies, but with secondary antibodies.

The primary antibodies used included: rabbit anti-NOP2 (sc-292098, 1:100 dilution; Santa Cruz Biotechnology, Dallas, TX); goat anti-POU5F1/OCT4 (sc-8628, 1:200 dilution; Santa Cruz Biotechnology, Dallas, TX); mouse anti-CDX2 (AM392-5M, 1:200 dilution; BioGenex, Fremont, CA); and rabbit anti-TP53 (#9284, 1:100 dilution; Cell Signaling Technology, Danvers, MA).

Statistical Analysis

All experiments were repeated at least three times. Student's t-test was used to evaluate the difference between groups, and a value of $P < 0.05$ was considered statistically significant. Data are expressed as mean ± standard error of the mean.

Acknowledgments

This work was supported in part by March of Dimes Research Grant #6-FY11-367 and NIH 1R21HD078942-01 to J Mager.

Abbreviations

dsRNA	double-stranded RNA
Nop2	nucleolar protein 2
RNAi	RNA interference

REFERENCES

Bantis A, Giannopoulos A, Gonidi M, Liossi A, Aggelonidou E, Petrakakou E, Athanassiades P, Athanassiadou P. Expression of p120, Ki-67 and PCNA as proliferation biomarkers in imprint smears of prostate carcinoma and their prognostic value. Cytopathology. 2004; 15:25–31. [PubMed: 14748788]

Biggers JD, Bell JE, Benos DJ. Mammalian blastocyst: Transport functions in a developing epithelium. Am J Physiol. 1988; 255:C419–C432. [PubMed: 3052100]

Blanco S, Frye M. Role of RNA methyltransferases in tissue renewal and pathology. Curr Opin Cell Biol. 2014; 31:1–7. [PubMed: 25014650]

Castello A, Fischer B, Eichelbaum K, Horos R, Beckmann BM, Strein C, Davey NE, Humphreys DT, Preiss T, Steinmetz LM, Krijgsveld J, Hentze MW. Insights into RNA biology from an atlas of mammalian mRNA-binding proteins. Cell. 2012; 149:1393–1406. [PubMed: 22658674]

Cockburn K, Rossant J. Making the blastocyst: Lessons from the mouse. J Clin Invest. 2010; 120:995–1003. [PubMed: 20364097]

de Beus E, Brockenbrough JS, Hong B, Aris JP. Yeast NOP2 encodes an essential nucleolar protein with homology to a human proliferation marker. J Cell Biol. 1994; 127:1799–1813. [PubMed: 7806561]

Fleming TP, Sheth B, Fesenko I. Cell adhesion in the preimplantation mammalian embryo and its role in trophectoderm differentiation and blastocyst morphogenesis. Front Biosci. 2001; 6:D1000–D1007. [PubMed: 11487467]

Gustafson WC, Taylor CW, Valdez BC, Henning D, Phippard A, Ren Y, Busch H, Durban E. Nucleolar protein p120 contains an arginine-rich domain that binds to ribosomal RNA. Biochem J. 1998; 331:387–393. [PubMed: 9531475]

Hong B, Brockenbrough JS, Wu P, Aris JP. Nop2p is required for pre-rRNA processing and 60S ribosome subunit synthesis in yeast. Mol Cell Biol. 1997; 17:378–388. [PubMed: 8972218]

Kosi N, Alic I, Kolacevic M, Vrsaljko N, Jovanov Milosevic N, Sobol M, Philimonenko A, Hozak P, Gajovic S, Pochet R, Mitrecic D. Nop2 is expressed during proliferation of neural stem cells and in adult mouse and human brain. Brain Res. 2015; 1597:65–76. [PubMed: 25481415]

Latham KE, Solter D, Schultz RM. Activation of a two-cell stage-specific gene following transfer of heterologous nuclei into enucleated mouse embryos. Mol Reprod Dev. 1991; 30:182–186. [PubMed: 1793594]

Marcho C, Cui W, Mager J. Epigenetic dynamics during preimplantation development. Reproduction. 2015; 150:R109–R120. [PubMed: 26031750]

Marikawa Y, Alarcon VB. Establishment of trophectoderm and inner cell mass lineages in the mouse embryo. Mol Reprod Dev. 2009; 76:1019–1032. [PubMed: 19479991]

Maserati M, Walentuk M, Dai X, Holston O, Adams D, Mager J. Wdr74 is required for blastocyst formation in the mouse. PLoS ONE. 2011; 6:e22516. [PubMed: 21799883]

Mitrecic D, Malnar T, Gajovic S. Nucleolar protein 1 (Nol1) expression in the mouse brain. Coll Antropol. 2008; 32:123–126. [PubMed: 18405070]

Perlaky L, Valdez BC, Busch RK, Larson RG, Jhiang SM, Zhang WW, Brattain M, Busch H. Increased growth of NIH/3T3 cells by transfection with human p120 complementary DNA and inhibition by a p120 antisense construct. Cancer Res. 1992; 52:428–436. [PubMed: 1728415]

Saijo Y, Sato G, Usui K, Sato M, Sagawa M, Kondo T, Minami Y, Nukiwa T. Expression of nucleolar protein p120 predicts poor prognosis in patients with stage I lung adenocarcinoma. Ann Oncol. 2001; 12:1121–1125. [PubMed: 11583194]

Schultz RM. The molecular foundations of the maternal to zygotic transition in the preimplantation embryo. Hum Reprod Update. 2002; 8:323–331. [PubMed: 12206467]

Stein P, Zeng F, Pan H, Schultz RM. Absence of nonspecific effects of RNA interference triggered by long double-stranded RNA in mouse oocytes. Dev Biol. 2005; 286:464–471. [PubMed: 16154556]

Svoboda P, Stein P, Hayashi H, Schultz RM. Selective reduction of dormant maternal mRNAs in mouse oocytes by RNA interference. Development. 2000; 127:4147–4156. [PubMed: 10976047]

Wang F, Yuan JH, Wang SB, Yang F, Yuan SX, Ye C, Yang N, Zhou WP, Li WL, Li W, Sun SH. Oncofetal long noncoding RNA PVT1 promotes proliferation and stem cell-like property of hepatocellular carcinoma cells by stabilizing NOP2. Hepatology. 2014; 60:1278–1290. [PubMed: 25043274]

Watson AJ, Damsky CH, Kidder GM. Differentiation of an epithelium: Factors affecting the polarized distribution of Na+, K(+)-ATPase in mouse trophectoderm. Dev Biol. 1990; 141:104–114. [PubMed: 2167855]

Wianny F, Zernicka-Goetz M. Specific interference with gene function by double-stranded RNA in early mouse development. Nat Cell Biol. 2000; 2:70–75. [PubMed: 10655585]

Yamanaka Y, Ralston A, Stephenson RO, Rossant J. Cell and molecular regulation of the mouse blastocyst. Dev Dyn. 2006; 235:2301–2314. [PubMed: 16773657]

Zeng F, Baldwin DA, Schultz RM. Transcript profiling during preimplantation mouse development. Dev Biol. 2004; 272:483–496. [PubMed: 15282163]

Zhang K, Dai X, Wallingford MC, Mager J. Depletion of Suds3 reveals an essential role in early lineage specification. Dev Biol. 2013a; 373:359–372. [PubMed: 23123966]

Zhang K, Haversat JM, Mager J. CTR9/PAF1c regulates molecular lineage identity, histone H3K36 trimethylation and genomic imprinting during preimplantation development. Dev Biol. 2013b; 383:15–27. [PubMed: 24036311]

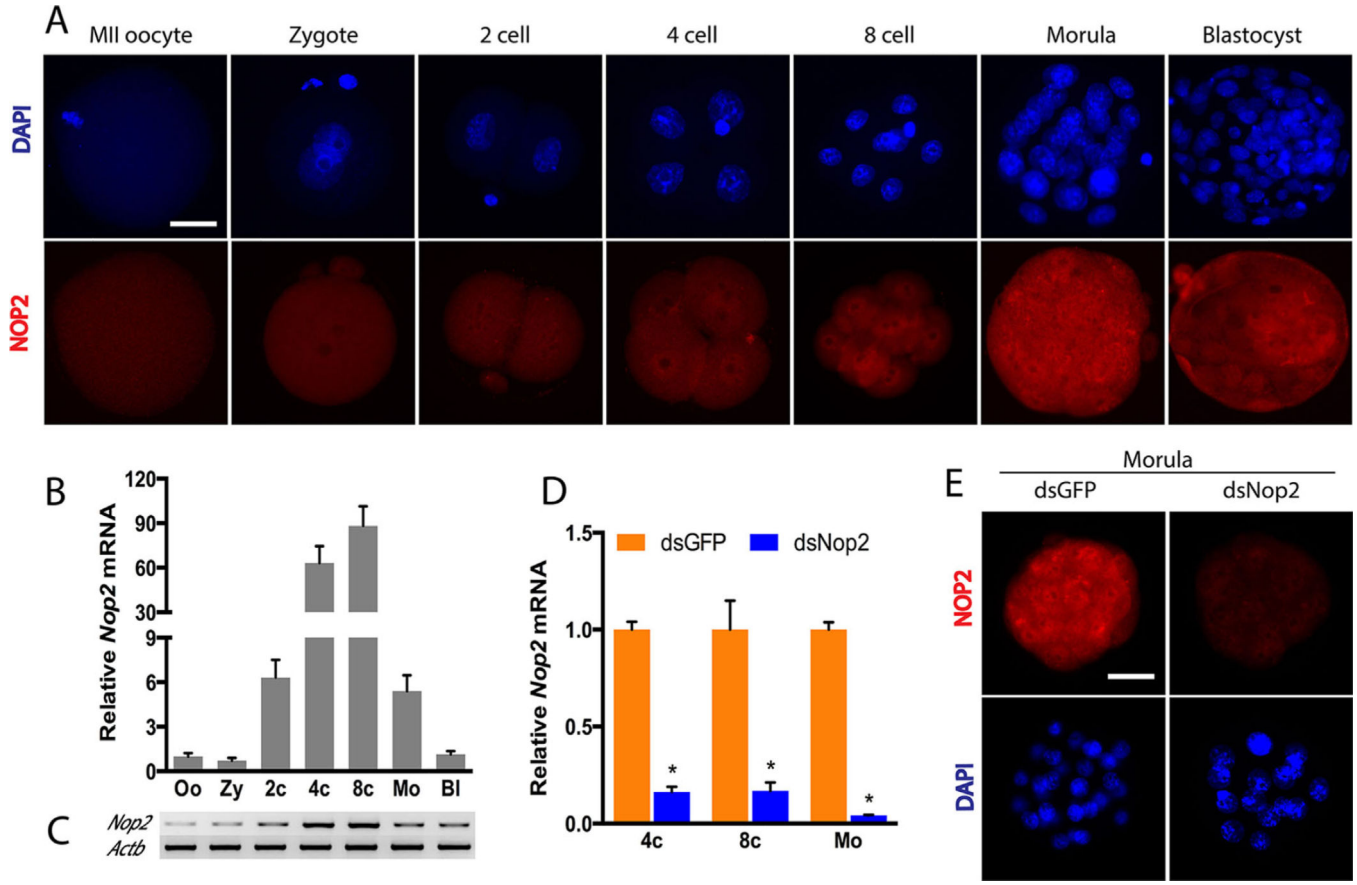

Figure 1.

Expression profile of *Nop2* during preimplantation development, and efficient knockdown of *Nop2* by dsNop2 RNA microinjection. **A**: Immunofluorescence analysis of NOP2 protein from the metaphase II (MII) oocyte to the blastocyst stage. Peak accumulation occurs at morula stage. **B** and **C**: Quantitative (B) and reverse-transcription (C) PCR for *Nop2* mRNA abundance in wild-type embryos during preimplantation development. **D**: Quantitative analysis of *Nop2* mRNA degradation following dsNop2 microinjection at the developmental stages examined.*, $P < 0.05$. Mean ± standard error is shown. **E**: Depletion of NOP2 protein in dsNop2 morula. Oo, MII oocyte; Zy, zygote; Mo, morula; Bl, blastocyst. Scale bar, 50 μm.

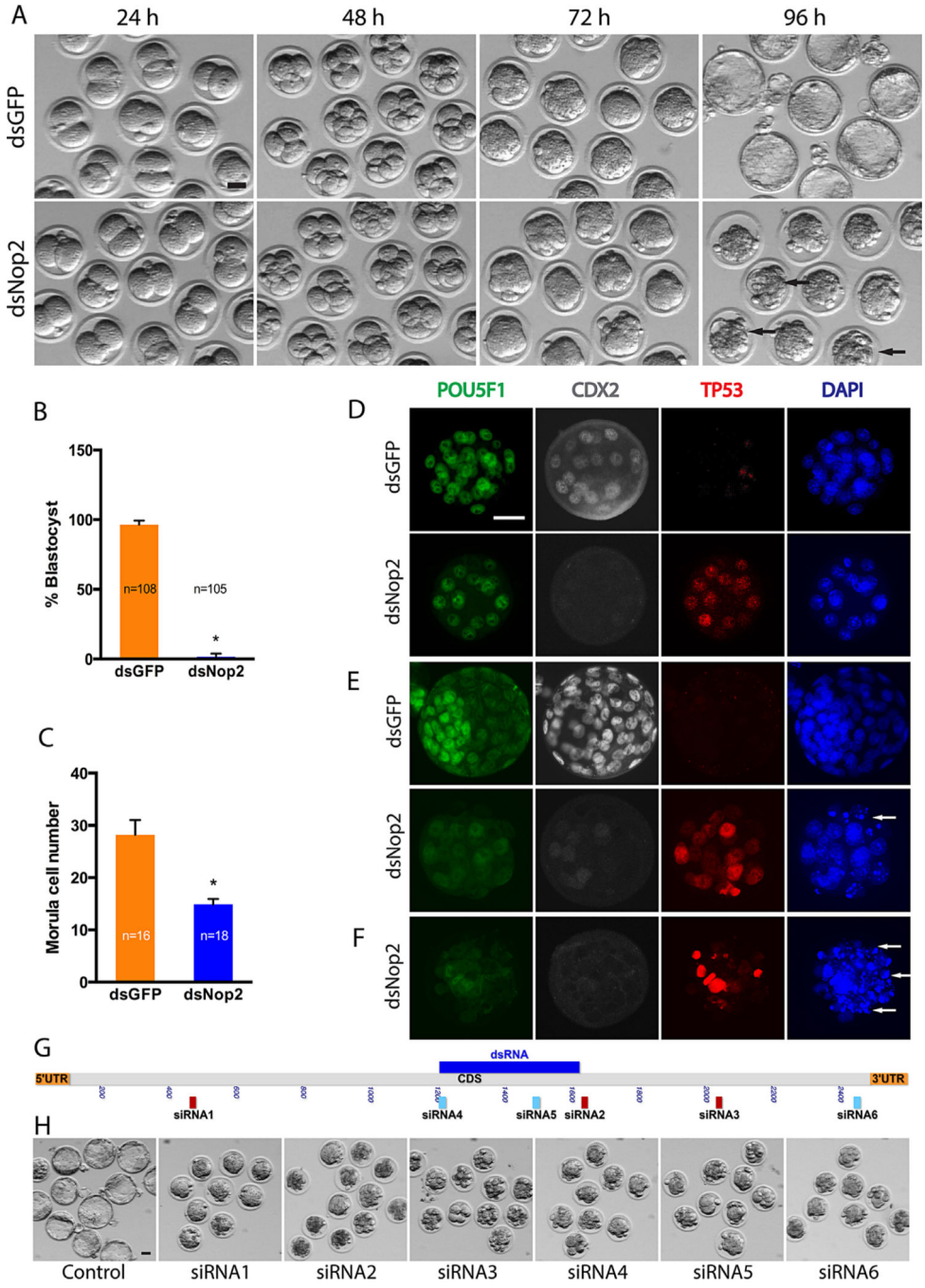

Figure 2.

Characterization of NOP2-deficient embryos. **A**: Developmental progression of dsNop2 embryos. Arrows indicate morphological abnormalities suggestive of degeneration. **B** and **C**: Blastocyst formation rate (B) and blastomere cell number (C) in the absence of NOP2. *, $P < 0.05$. Mean ± standard error is shown; "n" indicates the number of embryos examined. **D**–**F**: Immunofluorescence analysis of morula (D) and blastocysts (E) for the lineage-specific markers POU5F1 and CDX2 and the apoptotic marker activated TP53 in treated embryos at the expected times (D and E) or after extended culture (F). Cells with apoptotic bodies

(arrows) can be found in dsNop2 embryos. **G**: Schematic of *Nop2* mRNA (orange UTRs and grey CDs), with the target locations for the dsRNA (dark blue) and six distinct commercial siRNAs (red, Ambion; light blue, Qiagen) used to knockdown NOP2. **H**: Phenotype of siRNA-injected embryos. Most embryos injected with scrambled siRNA developed into blastocysts (11/12), whereas none of the embryos injected with one of the Nop2 siRNAs developed into blastocysts (0/69) (between 11 and 13 embryos were injected with each siRNA). Scale bar, 50 μm.

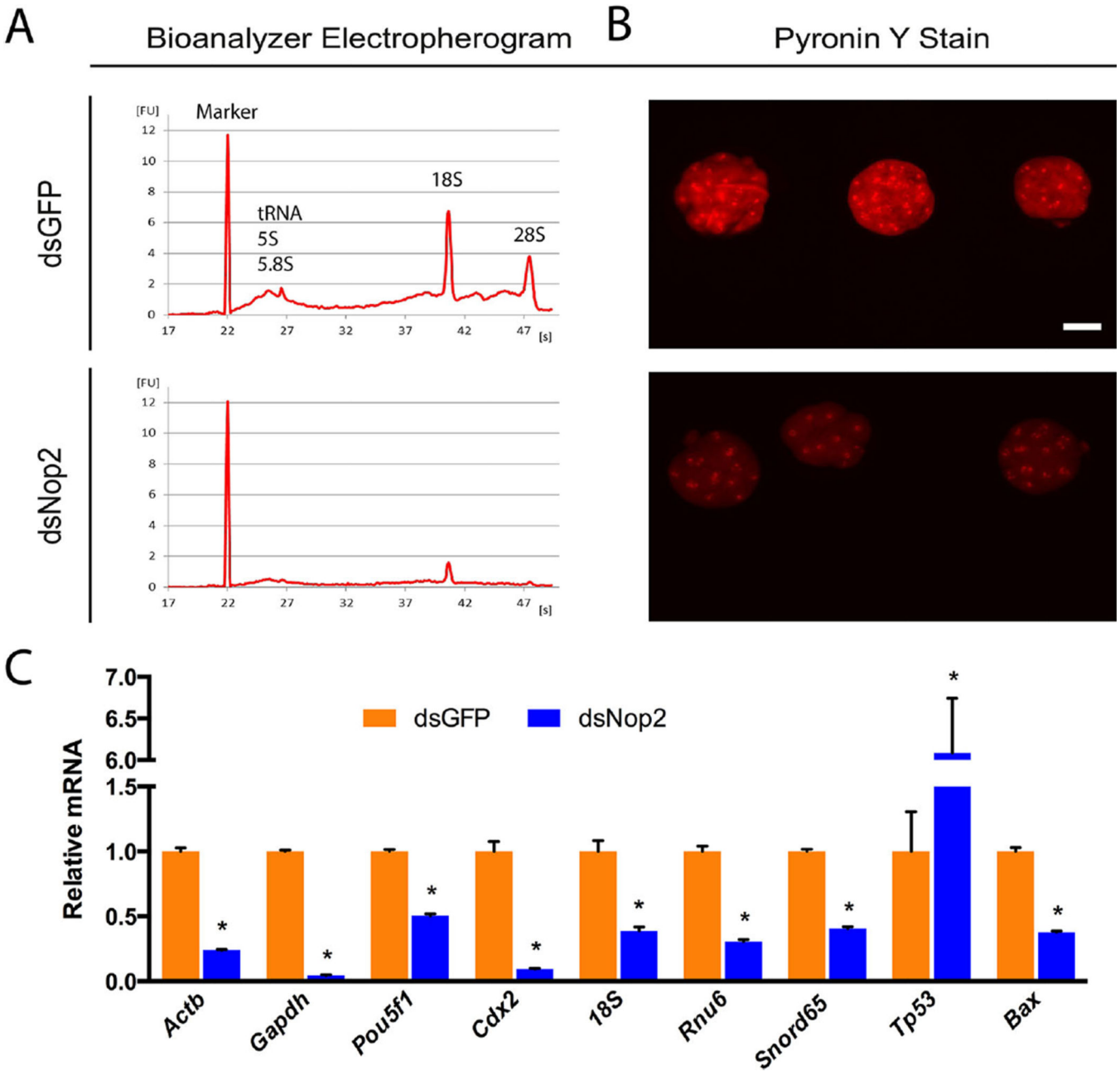

Figure 3.

Global RNA reduction in dsNop2 embryos. **A** and **B**: Bioanalyzer electropherograms (A) and Pyronin Y staining (B) of RNA after *Nop2* knockdown. Scale bar, 50 μm. **C**: Relative levels of different classes of RNA in injected embryos, representing rRNA (*18S*), small nuclear RNA (*Rnu6*), small nucleolar RNA (*Snord65*), and mRNAs (*Actb, Gapdh, Oct4, Cdx2, Bax*). *, $P < 0.05$. Mean ± standard error is shown.

TABLE 1

siRNA Sequences

Name	Sequence	Target location	Source	Catalog number
Scrambled	5′-CAGGGTATCGACGATTACAAA	n/a	Qiagen	1027280
Nop2 siRNA1	5′-GGACAGTGATGAAGATATG	460:478	Ambion	88181
Nop2 siRNA2	5′-CGAGTGGGTGGTAGACTAT	1627:1645	Ambion	173114
Nop2 siRNA3	5′-GGCTTGTCCACTGAACCTT	2027:2045	Ambion	173115
Nop2 siRNA4	5′-CAGGAGCATGAGCGGATCTTA	1202:1222	Qiagen	SI01328978
Nop2 siRNA5	5′-AAGACGAACAAGGATGAGAAA	1481:1501	Qiagen	SI01328992
Nop2 siRNA6	5′-AAGGAGGAAATCAATGACAAA	2437:2457	Qiagen	SI01328971